Journal of Applied Polymer Science

Size Controlling of Monodisperse Carboxymethyl Cellulose Microparticles via a Microfluidic Process

Yu Ke,[1] GuoSheng Liu,[2] Tianhui Guo,[1] Yi Zhang,[1] Chenghua Li,[1] Wei Xue,[1] Gang Wu,[3] Jiahui Wang,[4] Chang Du[3]

[1]Department of Biomedical Engineering, College of Life Science and Technology, Jinan University, Guangzhou 510632, China
[2]Department of Pediatrics, Institute of Fetal-Preterm Labor Medicine, The First Affiliated Hospital, Jinan University, Guangzhou 510632, China
[3]Biomaterial Research Institute, School of Materials Science and Engineering, South China University of Technology, Guangzhou 510641, China
[4]Biopolymer Division, National Engineering Research Center for Tissue Reconstruction and Restoration, Guangzhou 510006, China
Correspondence to: C. Du (E-mail: duchang@scut.edu.cn) and W. Xue (E-mail: weixue_jnu@aliyun.com)

ABSTRACT: Monodisperse carboxymethyl cellulose containing phenolic groups (CMC-Ph) microdroplets with a radius of 100–400 μm and a coefficient of variation below 3% were produced in a coflowing microfluidic device. The CMC-Ph solution containing horseradish peroxidase was used as the disperse phase and liquid paraffin containing H_2O_2 and lecithin as the continuous phase. The size of microdroplets decreased with the decreasing diameter of the inner channel and concentration of the disperse phase. When using a 0.04% CMC-Ph solution and the device with the inner diameter of 160 μm, the size of the microdroplets can be further controlled by the flow rates of both the continuous phase and disperse phase following exponential models. The volume of the microdroplet was not inversely proportional to the flow-rate ratio of the continuous phase to the disperse phase. There was a weak dependence of the volume on the flow of the continuous phase. The monodisperse microparticles possessed potential application for sensor, drug delivery system, cell encapsulation, catalysis, and imaging. © 2014 Wiley Periodicals, Inc. J. Appl. Polym. Sci. **2014**, *131*, 40663.

KEYWORDS: cellulose and other wood products; microfluidics; microgels

Received 17 September 2013; accepted 28 February 2014
DOI: 10.1002/app.40663

INTRODUCTION

Polymer-based microparticles have attracted considerable attention for applications including sensor, energy conversion and storage, drug delivery system, cell encapsulation, and imaging.[1–6] Various methods, such as mechanical stirring,[7] precipitation,[8] and layer-by-layer deposition,[9] are endeavored to prepare narrow-size-distributed microparticles. However, monodisperse microparticles with control over size, internal structure, and properties are in great demand for precisely quantifying the encapsulated substances. Recent advances in microfluid designs have brought the field of microfluidics to the forefront of the preparation of microparticles.[10–12] Over the conventional methods, microfluidics allows the production of microparticles in a consistent and controllable manner due to the characteristic laminar flow dynamics.[13]

The microdroplets prepared via microfluidic route can be gelled physically or chemically. Physical-crosslinking gels via ionic interactions are simple to be produced, but usually questioned by their reversibility.[14] The chemical crosslinking of gels has usually been achieved by crosslinker[15] or UV initiation,[16] however, the chemical initiator/crosslinker or UV light has potential harmful effect on the bioactivity of biomacromolecules encapsulated. Enzymatic reaction has recently attracted much attention due to its low toxicity, mild reaction, stereochemistry, high reaction velocity, high enantio-, regio-, and chemo-selectivity.[17] Horseradish peroxidise/hydrogen peroxide (HRP/H_2O_2) is a common enzymatic system, where peroxidases functioned as oxidoreductases to catalyze the oxidation of donors using H_2O_2.

Polysaccharides with phenolic groups (Ph) for HRP-catalyzed gelation of microdroplets via microfluidic route, such as hyaluronic acid,[18] alginate,[19] dextran[20] or chitosan,[21] have been synthesized by conjugating with tyramine that is usually found in ripe cheese, wine and fermented or aged foods. Compared with these polysaccharides, the easily available carboxymethyl cellulose (CMC) with high purity and low cost is very attractive.[22] CMC has much application for food, cosmetic and pharmaceutical or biomedical products owing to its water-solubility,

biodegradability, and biocompatibility.[23] Sakai et al. have attempted to modify CMC with tyramine,[24] and then prepared cell-laden CMC microspheres on a microfluidic device via HRP/H_2O_2,[25] demonstrating a good model for the encapsulation of live cells.

The 4-Hydroxybenzylamine, having primary amine and hydroxyl groups on both ends, respectively, is an intermediate used for synthesizing medicine or functional material. In this study, we synthesized a 4-hydroxybenzylamine modified CMC (CMC-Ph) and prepared monodispersed CMC-Ph microdroplets of tunable radius ranging from 100 to 400 μm via a microfluidic device. As far as we know, CMC modified with 4-hydroxybenzylamine has not been reported by other labs. In the microfluidic device, the aqueous CMC-Ph solution (the dispersed phase) was infused through the inner microchannel into coflowing liquid paraffin containing H_2O_2 and lecithin (the continuous phase) to form CMC-Ph emulsion that was then solidified through enzymatic reaction. The mean radius of the CMC-Ph microparticles and the coefficients of variation (CV) were calculated. We detailed the dependencies of droplet size on changes in channel dimension, polymer concentration, and flow rates, and discussed a model of the size of CMC-Ph microdroplets.

MATERIALS AND METHODS

Materials

1-Ethyl-3-(3-dimethylaminopropyl)carbodiimide hydrochloride (EDC), *N*-hydroxysulfosuccinimide (NHS), HRP (250 units/mg), lecithin, 4-hydroxybenzylamine, 1-hydroxybenzotriazole hydrate (HOBT), and 2-(4-morpholino)ethanesulfonic acid (MES) were obtained from Qiyun Biotech (China). Aqueous H_2O_2 (30%, w/w) and liquid paraffin were purchased from Dalu Chemical Reagent (China). All reagents were analytical grade and used as received.

CMC with weight-average molecular weight (M_w) of 1.0×10^5 was purchased from Jingchun Chemical Reagent (China). CMC-Ph was synthesized as following: CMC was dissolved in 300 mL of MES buffer (50 m*M*, pH 6.0) at 1.0 % (w/v) and stirred for 30 minutes at 25°C to prepare a clear CMC solution. 4-Hydroxybenzylamine was added to the solution at a weight ratio of 1 : 0.56 (CMC:4-hydroxybenzylamine) and stirred for 20 minutes. NHS, HOBt, and EDC were then added in order at a weight ratio of 1 : 0.26 : 0.68 : 0.70 (CMC : NHS : HOBt : EDC). The mixture was magnetic stirred for 24 hours and then dialyzed against deionized water using an ultrafiltration membrane (molecular weight cutoff = 3500 Da) at 25°C. In the process of dialysis, the existing water was replenished every 2–4 hours. Four days later, the resultant polymer solution was enriched by a rotary evaporator (100 rpm) at 50°C, frozen at −20°C overnight, and subsequently lyophilized (−65°C, 6 pa) for 12 hours.

Preparation of CMC-Ph Microparticles

Microfluidic devices with diameters of 160, 260, and 340 μm for the inner channel were used for preparing CMC-Ph microparticles, respectively. Two immiscible fluids, the dispersed phase and the continuous phase, were injected into the devices using microsyringe pumps (Baoding Longer TS-1B/W0109-1B, China). CMC-Ph was dissolved in ultrapure water containing HRP (10 units/mL) as the dispersed phase. The continuous liquid paraffin phase containing H_2O_2 and lecithin was prepared as follows: 1.25 mL of aqueous H_2O_2 was added into 250 mL of liquid paraffin. The mixture was magnetically stirred for 12 hours at 25°C and centrifuged at 2000 rpm for 10 minutes. The lower aqueous H_2O_2 solution was discarded. Then, lecithin (droplet stabilizer) was dissolved at 3.0% (w/v) into the collected upper liquid paraffin containing H_2O_2. In the microfluidic devices, the dispersed phase was slowly injected into the inner channel, while the continuous phase was injected into an inlet in a perpendicular direction and flowed along the space between the inner and outer channel. The pressure-driven flow of the dispersed liquid subsequently broke into equal-sized droplets at the end of the inner channel.

Characterization

Rheological behavior of CMC-Ph solutions with different concentrations was measured by using a TA ARES/RFS rotational viscometer at 30°C. The employed shear rate varied from 0.01 to 250 s^{-1}, and viscosity or stress was identified. The solutions were prepared by mass using a XS105DU balance (Mettler Toledo, Switzerland) with a precision of 10^{-5} g.

Density of CMC-Ph solution was determined using 25 cm^3 of Gay-Lussac pycnometer. The pycnometer containing the solution was thermostated to maintain at 30°C. The density was calculated according to the following formula:

$$\rho_2 = \frac{m_2 - m_0}{m_1 - m_0}\rho_1 \quad (1)$$

where m_0 is the mass of the empty pycnometer, m_1 is the mass of the pycnometer full of the reference solution, m_2 is the mass of the pycnometer full of CMC-Ph solution, ρ_1 is the density of the reference solution, ρ_2 is the density of CMC-Ph solution. Each density value was the average of five measurements.

A SMZ-DM200 stereomicroscope (Optec, China) equipped with a color CCD camera was used to record the formation of the microdroplets. Images were downloaded digitally, and the number-average diameters and coefficients of variation (CV, defined as the ratio of standard deviation to the mean) were characterized by analyzing optical microscopy images of 100 particles.

$$CV = \left(\sum_{i=1}^{n}\left[(di - \overline{d})^2/n\right]\right)^{1/2} / \overline{d} \quad (2)$$

Where *di* was the diameter of the *i*th microdroplet, *n* was the total number of the microdroplets counted (100), and $\overline{d}$ was the average diameter.

RESULTS AND DISCUSSION

Schematic Microfluidic Process

CMC-Ph was synthesized through EDC/NHS coupling agents. Figure 1(a) presents the chemical structure of CMC-Ph with the grafted phenolic groups that had a characteristic UV absorbance peak at 275 nm.[26] CMC-Ph microdroplets were prepared via a microfluidic process. When CMC-Ph solution was injected into

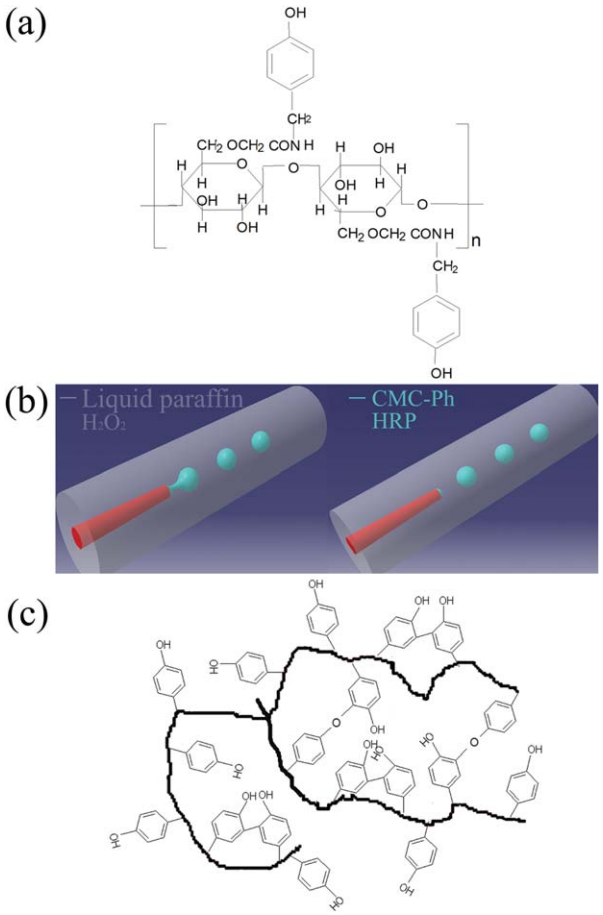

Figure 1. Schematic drawing of the formation of CMC-Ph microgels: (a) Chemical structure of CMC-Ph; (b) Microfluidic process of the formation of CMC-Ph microdroplets; (c) Chemical structure of CMC-Ph microgels. [Color figure can be viewed in the online issue, which is available at wileyonlinelibrary.com.]

a flow of liquid paraffin, it was axisymmetrically pinched by the continuous flow, resulting in the elongation of the CMC-Ph streams [Figure 1(b), left], which spontaneously separated and broke up into microdroplets [Figure 1(b), right]. Series of controlled break-up of the coaxial fluids led to the production of highly monodisperse microdroplets.

Once the CMC-Ph droplets were in contact with the continuous phase (H_2O_2/liquid paraffin emulsion), the micelle around the droplets would aggregate and form an interphase between water (microdroplets and H_2O_2) and oil (the continuous fluid). Then, H_2O_2 would diffuse into the aqueous phase and the CMC-Ph microdroplets solidified into a gel afterward via the enzymatic reaction [Figure 1(c)], resulting in polyphenols linked at the aromatic ring by C—C and C—O coupling of phenols.[27] The sustaining diffusion of H_2O_2 from the continuous phase to the droplets caused the gelation of the microgels in the followed downstream channels.

It is usually believed that the Rayleigh-Plateau hydrodynamic instability arising in the channel between the dispersed and continuous phases is effectively combined for the formation of monodisperse droplets. The mechanism of drop formation is a balance of interfacial tension and the shear of the continuous phase acting on the dispersed phase.[28,29] Two dimensionless numbers that significantly contribute to the final droplet diameter are identified, Capillary number ($C_a = \mu\upsilon/\gamma$) and Reynolds number ($R_e = \rho\upsilon d/\mu$), where μ is the viscosity, υ is the flow rate, γ is the interfacial tension, ρ is the density, and d is the equivalent diameter. Viscosity and density of CMC-Ph solution with different concentration has been illustrated in Table I. CMC-Ph solution with the concentration in 0.02–1.00% range showed a Newtonian characteristic, although the CMC solution is believed to be a typical non-Newtonian fluid.[30,31]

Controlled Preparation of CMC-Ph Microparticles on Three Microfluidic Devices

Figure 2 illustrates the light microscope images of the microdroplets being formed in the microfluidic devices with the different diameters of inner channels along with the size distribution. CMC-Ph solution (0.04%) was injected at a flow rate of 10 μL/min (Q_d), and the rate of continuous phase (Q_c) was fixed at 10 mL/min. In these microfluidic devices, liquid paraffin was selected as the continuous phase because it was inert and immiscible with the CMC-Ph solution. The resulted microdroplets were in round shape with smooth surface, and coalescence was absent in a well-controlled flow field [Figure 2(a–c)].

The mean size and size distribution of the microdroplets were calculated based on the images. As the diameter of inner channel increased, the radius of microdroplets increased significantly from 116.87 ± 1.47 μm to 186.15 ± 2.75 μm. The size distribution of the microdroplets was unimodal with CVs less than 3%, illustrating good monodispersity in size.[32] The Capillary number and Reynolds number of the disperse fluids (C_{ad} and R_{ed}) and of the continuous fluids (C_{ac} and R_{ec}) were presented in Table II. R_{ed} and R_{ec} were quite low, in order to ensure stable laminar flows. The C_{ad} and C_{ac} increased as the diameter of the channel decreased. Usually, a reduction in the characteristic dimension of the microfluidic system generates smaller particles, which is one of the most efficient routes to a reduction in microdroplets diameter.[33] The microfluidic device with the

Table I. Viscosity and Density of the Disperse and the Continuous Liquids

Sample	CMC-concentration (wt %)	Viscosity (pa·s)	Density (g/cm^3)
Disperse fluid	0.02	0.0011	0.9992
	0.04	0.0015	0.9990
	0.20	0.0028	0.9991
	0.40	0.0031	1.0016
	0.60	0.0041	1.0023
	0.80	0.0047	1.0032
	1.00	0.0054	1.0034
Continuous fluid	-	0.0330	0.8650

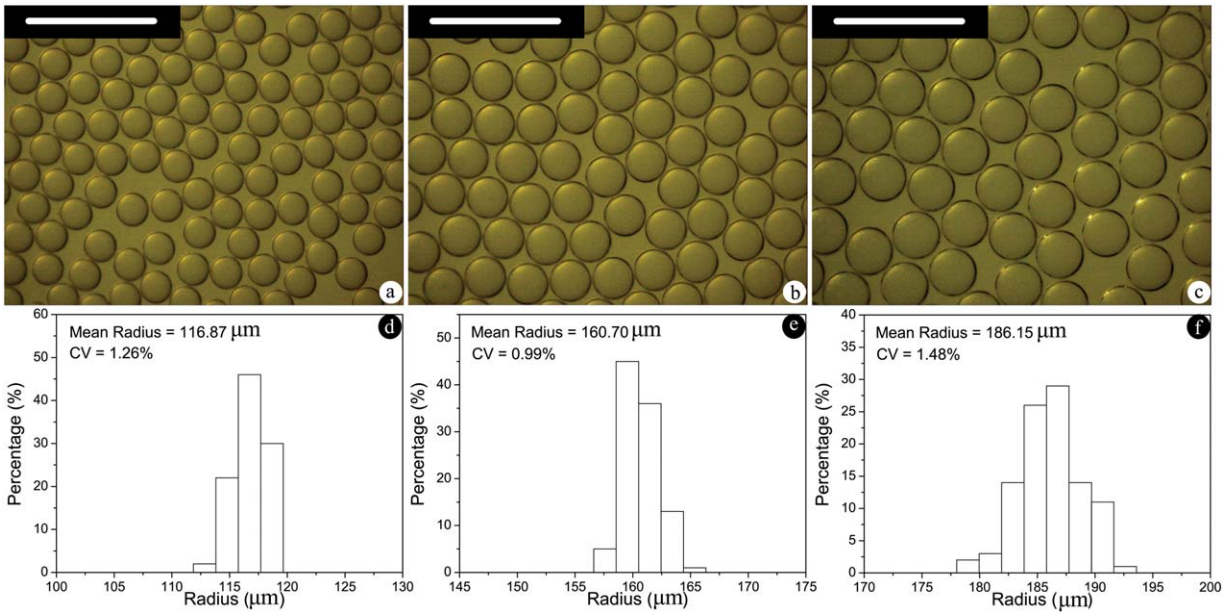

Figure 2. Micrographs of the CMC-Ph microparticles being formed in the microfluidic devices with different inner-channel diameters and the size distribution: (a,d) 160 μm; (b,e) 260 μm; (c,f) 340 μm. CMC-Ph concentration = 0.04%, Q_d = 10 μL/min, Q_c = 10 mL/min. Scale bar = 500 μm. [Color figure can be viewed in the online issue, which is available at wileyonlinelibrary.com.]

inner-channel diameter of 160 μm (Device 1) was used for following studies.

Tunability of CMC-Ph Microparticles Size on the Concentration of the Dispersed Fluid

Figure 3(a) presents the size of the CMC-Ph microdroplets, being obtained at Q_d = 10 μL/min, Q_c = 10 mL/min. As the concentration of the CMC-Ph solution increased from 0.04% to 5.0%, the radius of the CMC-Ph microdroplets increased, in concordance with the argument that highly viscous liquids were emulsified into larger droplets.[34] The result clearly showed that the concentration of CMC-Ph solution had great effect on the size of CMC-Ph microdroplets.

The microparticles (5% CMC-Ph) containing black ink as an indicator were prepared and centrifuged at 2000 rpm for 10 minutes. The isolated microparticles were then removed from the continuous phase into water, as shown in Figure 3(b). The microparticles swelled and their diameter was 1.7 times of those in the continuous phase. Although carbon black was not well distributed, it could be clearly seen that the swollen CMC-Ph microgels maintained round shape due to the HRP-H_2O_2 cross-linking reaction.

Flow Rates-Dependence of the Size of CMC-Ph Microparticles

For a given solution, the dynamics of the breakup in a confined geometry of a microfluidic device can be easily controlled by Q_c and Q_d at the point where the breakup occurs. We snapped the droplets just before the breakup (Figure 4). When Q_d and Q_c were 10 μL/min and 2 mL/min, respectively, two droplets coexisted along the flow direction with a distinct interface (a). As Q_d increased over 60 μL/min (b,c), no coexisting of droplets presented. One large droplet was pushed forward with a small column in the end. When Q_c increased at a fixed Q_d (10 μL/min), a slim column presented (d) and diminished gradually when Q_c was over 6 mL/min (e, f). The morphology of droplets just before the breakup was quite different. Round-shape droplets hung on the outlet at the increased Q_d, whereas the stretching droplets appeared at the increased Q_c. Once flowed away from the outlet, the stretching droplets recovered into round-shape.

The gap between the droplets is a crucial parameter because it determines the yield of the CMC-Ph microdroplets. Also, proper gap is imperative to prevent coalescence among the fresh droplets. The flow rates of the disperse fluid and the continuous fluid were controlled properly by two independent syringe pumps to obtain independent droplets with a stable periodic generation. The resulting uniform microdroplets with identical gaps flowed along the channel (Figure 5). The gap increased as the flow rate of the continuous phase increased (a_1–c_1, Q_d = 120 μL/min), with the frequency of generation was 95, 106, and 137 droplets per minute, respectively. As the flow rate of the dispersed phase decreased from 120 μL/min to 60 μL/min, the gap increased (a_2–c_2, Q_c = 2 mL/min), while the amount of droplets per minute decreased to 80 (Q_d = 90 μL/min) and 61 (Q_d = 60 μL/min).

Table II. C_a and R_e of the Disperse and Continuous Fluids in Three Microfluidic Devices

Microfluidic device	Diameter of inner-channel (μm)	C_{ad} ($\times 10^4$)	R_{ed}	C_{ac}	R_{ec}
Device 1	160	2.57	0.87	2.03	24.40
Device 2	260	0.97	0.54	0.74	14.70
Device 3	340	0.57	0.41	0.49	12.08

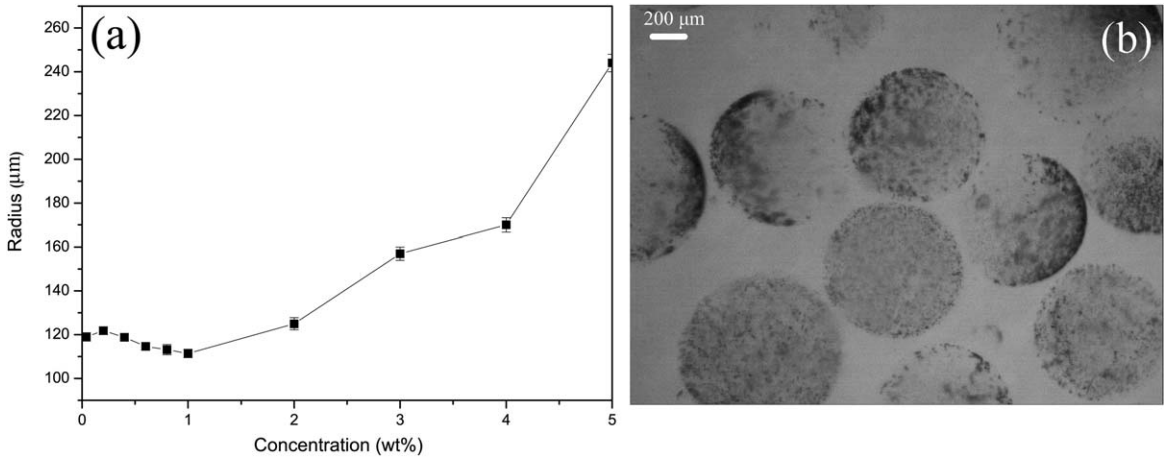

Figure 3. (a) Size of CMC-Ph microparticles being prepared with different CMC-Ph concentration ($Q_d = 10$ μL/min, $Q_c = 10$ mL/min); (b) Micrograph of CMC-Ph microgels in water, Scale bar = 200 μm. (CMC-Ph concentration = 5%, $Q_d = 10$ μL/min, $Q_c = 10$ mL/min).

The variation in size was quantified by the changes in Q_c, while fixing Q_d at 2 μL/min. As shown in Figure 6(a), the microdroplets being prepared by 0.04% CMC-Ph ($C_{ad} = 0.515 \times 10^{-4}$, $R_{ed} = 0.174$) showed maximum radium of 377.80 ± 4.17 μm at $Q_c = 0.5$ mL/min, which dropped to 93.17 ± 1.95 μm when Q_c increased to 15 mL/min. As Q_c increased, C_{ac} and R_{ec} increased

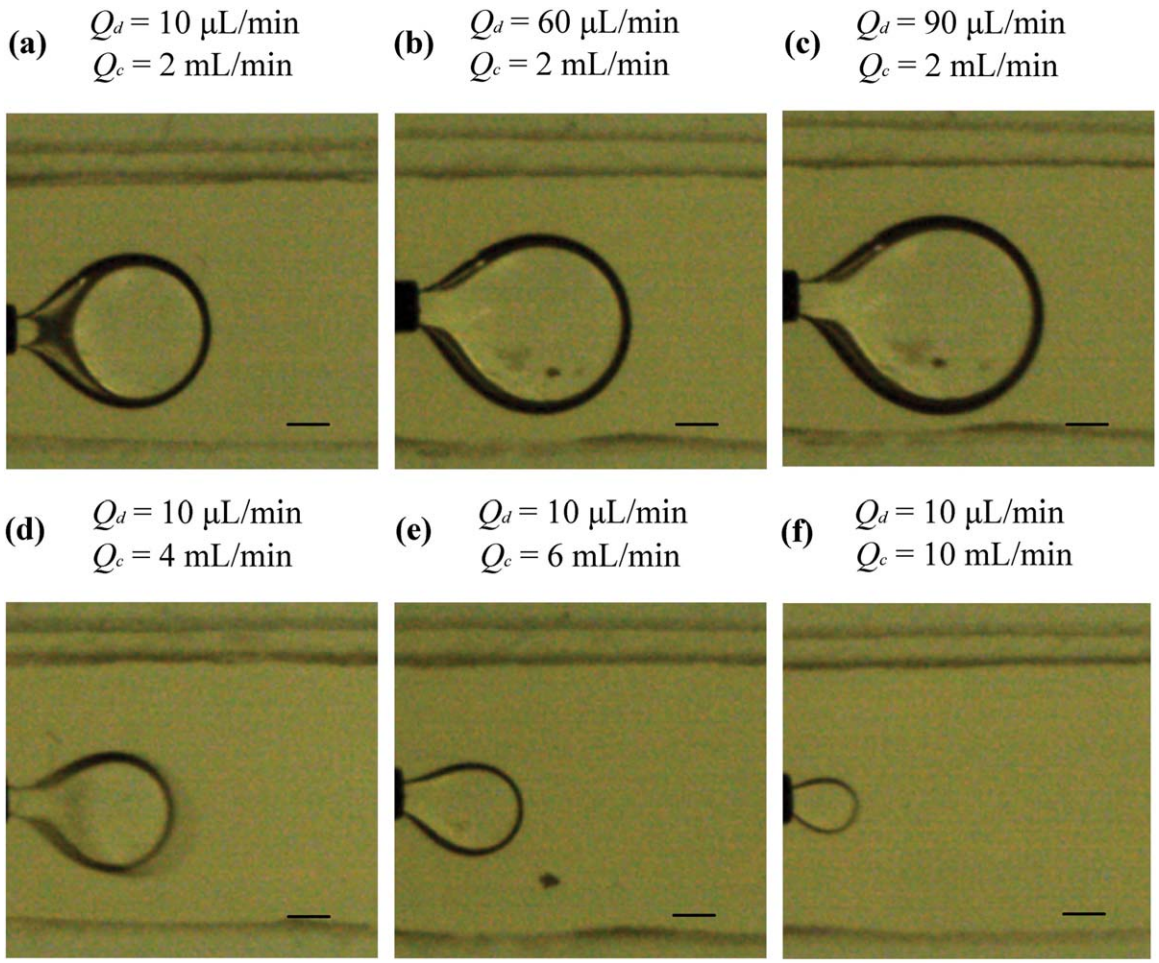

Figure 4. Snapshots of the breakup of the droplets under different hydrodynamic conditions: (a) $Q_d = 10$ μL/min, $Q_c = 2$ mL/min; (b) $Q_d = 60$ μL/min, $Q_c = 2$ mL/min; (c) $Q_d = 90$ μL/min, $Q_c = 2$ mL/min; (d) $Q_d = 10$ μL/min, $Q_c = 4$ mL/min; (e) $Q_d = 10$ μL/min, $Q_c = 6$ mL/min; (f) $Q_d = 10$ μL/min, $Q_c = 10$ mL/min. Scale bar = 200 μm. [Color figure can be viewed in the online issue, which is available at wileyonlinelibrary.com.]

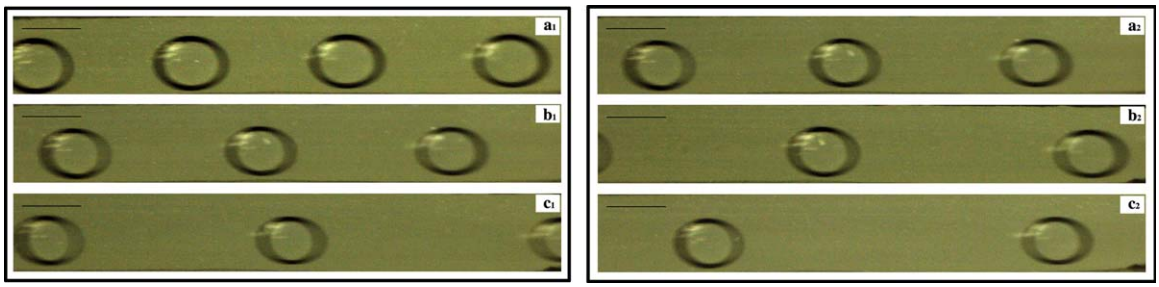

Figure 5. Snap photographs of the separated microdroplets produced along the channels. (1) Effect of Q_c on the gap of the microdroplets ($Q_d = 120$ μL/min): (a_1) $Q_c = 1.5$ mL/min; (b_1) $Q_c = 2.0$ mL/min; (c_1) $Q_c = 2.5$ mL/min; (2) Effect of Q_d on the gap of the microdroplets ($Q_c = 2$ mL/min): (a_2) $Q_d = 120$ μL/min; (b_2) $Q_d = 90$ μL/min; (c_2) $Q_d = 60$ μL/min. Scale bar = 500 μm. [Color figure can be viewed in the online issue, which is available at wileyonlinelibrary.com.]

and fell in the range of 1.01–30.42 and 12.20–365.98, respectively. Similarly, the radium of microdroplets being prepared by 1.00% CMC-Ph decreased from 472.73 ± 5.53 μm to 165.00 ± 3.08 μm. As expected, an increase in flow rate of continuous fluids resulted in smaller microdroplets at a fixed CMC-Ph flow rate.[35] The flow rate of the continuous phase affected the size of the microdroplets according to exponential models as eqs. (3) and (4), respectively, for 0.04% and 1.00% CMC-Ph samples.

$$Y = 321.4 \exp(-X/3.3) + 92.7 \left(R^2 = 0.9968\right) \quad (3)$$

$$Y = 345.7 \exp(-X/3.8) + 159.2 \left(R^2 = 0.9973\right) \quad (4)$$

X: flow rate of the continuous phase, Y: radius of CMC-Ph microdroplets.

Microdroplets size as a function of the flow rate of the disperse phase was shown in Figure 6(b). The microdroplets were prepared by using 0.04% or 1.00% CMC-Ph solution as the dispersed fluids and fixing Q_c at 10 mL/min. By changing Q_d from 0.75 μL/min to 60 μL/min for 0.04% CMC-Ph sample ($C_{ac} = 2.028$, $R_{ed} = 24.398$), we obtained microdroplets with radius from 106.71 ± 2.42 μm to 151.42 ± 2.55 μm. When Q_d went up, C_{ad} increased from 0.19×10^{-4} to 46.31×10^{-4}, and R_{ed} from 0.07 to 15.70, respectively. For 1.00% CMC-Ph sample, the radius of microdroplets increased from 157.44 ± 3.15 μm to 237.22 ± 3.85 μm, as Q_d increased from 2 μL/min to 50 μL/min. The exponential eqs. (5) and (6) are respectively for 0.04% and 1.00% CMC-Ph samples.

$$Y = -54.2 \exp(-X/31.6) + 159.3 \left(R^2 = 0.9824\right) \quad (5)$$

$$Y = -86.2 \exp(-X/16.3) + 240.7 \left(R^2 = 0.9728\right) \quad (6)$$

X: flow rate of the dispersed phase, Y: radius of CMC-Ph microdroplets

Model of the Size of CMC-Ph Microparticles

According to the rate-of-flow-controlled break-up mechanism, the volume of the microdroplet (V) is inversely proportional to the ratio of the flow rates: $V \propto (Q_c/Q_d)^{-1}$.[29] In this formula, the volume of a microdroplet was calculated as $V = (4/3)\pi(R)^3$, where R is the radius of the microdroplet. The dependence of the droplet-volume on the flow-rate ratios was monitored as the flow rate of the continuous fluid (open square, □) or the disperse fluid (closed square, ■) was kept constant [Figure 7(a)]. The increase in the flow-rate ratio of the continuous fluid to the disperse fluid resulted in a decrease in droplet size, perhaps due to the increasing shear stress imposed on the disperse fluid. Obviously, the rate-of-flow-controlled break-up model did not predict the volume of the microdroplet well.

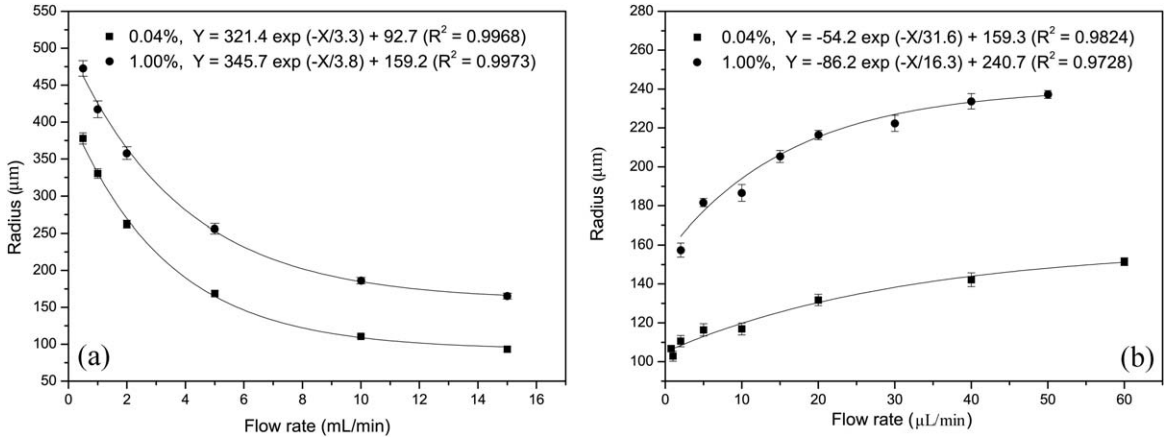

Figure 6. Relationship between flow rates and microdroplets size obtained by using the CMC-Ph concentration of 0.04% and 1.00%: (a) Effect of Q_c on the radius of microdroplets at a constant Q_d (2 μL/min); (b) Effect of Q_d on the radius of microdroplets at a fixed Q_c (10 mL/min).

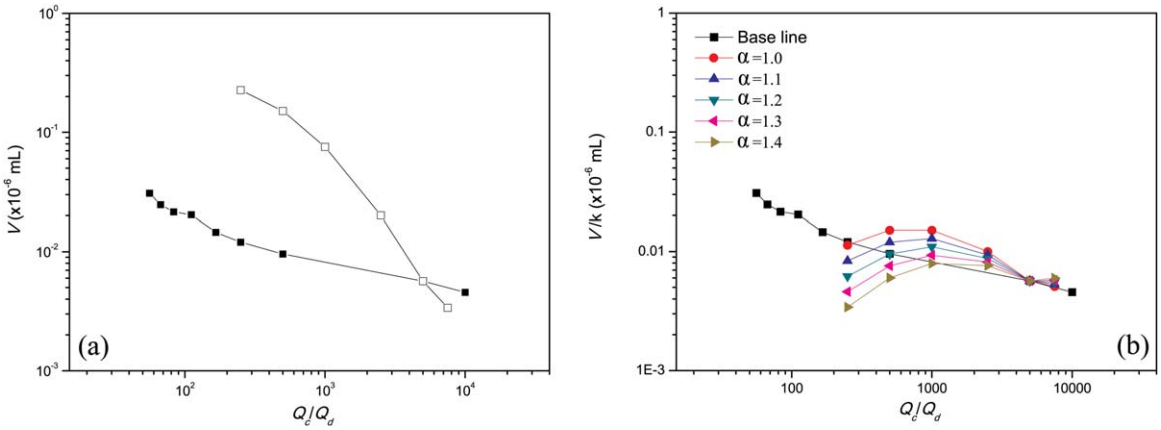

Figure 7. Dependence of the flow rate ratios on the volume of the microdroplets (a) and on the volume of the microdroplets devided by the correction index k (b). CMC-Ph microdroplets were obtained at CMC-Ph concentration (0.04%) and inner-channel diameter (160 μm): (■) $Q_c = 10$ mL/min, $Q_d = 0.75 \sim 180$ μL/min; (□) $Q_d = 2$ μL/min, $Q_c = 0.5 \sim 15$ mL/min. [Color figure can be viewed in the online issue, which is available at wileyonlinelibrary.com.]

The shearing mechanism relates to the diameter of the droplet to the reciprocal of the capillary number, which yields a much stronger dependence on the ratio of the rates of flow $V \propto (Q_c/Q_d)^{-3}$. Stone and coworkers have suggested that low viscosity fluids break up according to the rate-of-flow-controlled mechanism, whereas the fluids of higher viscosity gradually depart from this model, showing gradually weaker dependence of the volume of droplets on the rates of the continuous fluid.[34] Therefore, we introduced a correction index, a relative ratio of two flow rates of the continuous fluids $k = (Q_{c■}/Q_{c□})^{\alpha}$, to examine the role of the flow rate of the continuous fluid in the break-up process. The dependence of V/k on Q_c/Q_d ratio (250–7500) was evaluated [Figure 7(b)]. The curve being obtained at $Q_{c■}$ of 10 mL/min was chosen as a base line (■), and $Q_{c□}$ was altered from 0.5 to 15 mL/min. When α altered from 1.1 to 1.4, the corrected data got close to the base line, showing a weak dependence of the droplet-volume on the flow rate of the continuous fluid.

CONCLUSIONS

Monodisperse CMC-Ph microdroplets were obtained in the coflowing microfluidic devices. The radius was tuned in the range of 100 to 400 μm by changing the dimension of the microchannels, CMC-Ph properties, and the flow rates of the disperse phase and the continuous phase. As the diameter of the inner channel or the concentration of CMC-Ph decreased, the size of microparticles decreased. The flow rates of the continuous phase and the dispersed phase affected the size of the microdroplets according to the exponential models. The break-up process did not fully fit the rate-of-flow-controlled mechanism, and showed a weak dependence of the droplet-volume on the flow rate of the continuous fluid. CMC-Ph could be used to produce monodisperse microparticles with precise control over their sizes, size distributions, and morphologies, which might encapsulate drug, cell, catalyst or tracer for biomedical application.

ACKNOWLEDGMENTS

This study was financially supported by the Basic Research Project of China (2012CB619105), the National Natural Science Foundation of China (51072056, 51173053), Guangdong Natural Science Foundation (9451063201003024), Guangdong Provincial Program for Excellent Talents in Universities, and Key Laboratory of Biomaterials of Guangdong Higher Education Institutes of Jinan University.

REFERENCES

1. Peeters, M.; Troost, F. J.; van Grinsven, B.; Horemans, F.; Alenus, J.; Murib, M. S.; Keszthelyi, D.; Ethirajan, A.; Thoelen, R.; Cleij, T. J.; Wagner, P. *Sensor. Actuat. B-Chem.* **2012**, *171*, 602.
2. Phadungphatthanakoon, S.; Poompradub, S.; Wanichwecharungruang, S. P. *ACS. Appl. Mater. Inter.* **2011**, *3*, 3691.
3. Zhang, L.; Jeong, Y. I.; Zheng, S.; Suh, H.; Kang, D. H.; Kim, I. *Langmuir* **2013**, *29*, 65.
4. Tekin, H.; Tsinman, T.; Sanchez, J. G.; Jones, B. J.; Camci-Unal, G.; Nichol, J. W.; Langer, R.; Khademhosseina, A. *J. Am. Chem. Soc.* **2011**, *133*, 12944.
5. Wu, B.; Gong, H. Q. *Microfluid. Nanofluid.* **2012**, *13*, 909.
6. Ke, Y. *Recent Pat. Biomed. Eng.* **2012**, *5*, 223.
7. Weng, L. H.; Le, H. C.; Lin, J. Y.; Golzarian, J. *Int. J. Pharmaceut.* **2011**, *409*, 185.
8. Kulterer, M. R.; Reichel, V. E.; Kargl, R.; Kostler, S.; Sarbova, V.; Heinze, T.; Stana-Kleinschek, K.; Ribitsch, V. *Adv. Funct. Mater.* **2012**, *22*, 1749.
9. Qi, A.; Chan, P.; Ho, J.; Rajapaksa, A.; Friend, J.; Yeo, L. *ACS Nano* **2011**, *5*, 9583.
10. Dendukuri, D.; Doyle, P. S. *Adv. Mater.* **2009**, *21*, 4071.
11. Lazarus, L. L.; Riche, C. T.; Marin, B. C.; Gupta, M.; Malmstadt, N.; Brutchey, R. L. *ACS Appl Mater. Interfaces* **2012**, *4*, 3077.
12. Ke, Y. *Recent Pat. Nanomed.* **2011**, *1*, 109.
13. Utada, A. S.; Lorenceau, E.; Link, D. R.; Kaplan, P. D.; Stone, H. A.; Weitz, D. A. *Science* **2005**, *308*, 537.

14. Zhang, H.; Tumarkin, E.; Peerani, R.; Nie, Z. H.; Sullan, R. M. A.; Walker, G. C.; Kumacheva, E. *J. Am. Chem. Soc.* **2006**, *128*, 12205.
15. Marquis, M.; Renard, D.; Cathala, B. *Biomacromolecules* **2012**, *13*, 1197.
16. Seiffert, S.; Romanowsky, M. B.; Weitz, D. A. *Langmuir* **2010**, *26*, 14842.
17. Kobayashi, S.; Uyama, H.; Kalra, B. *Chem. Rev.* **2001**, *101*, 3793.
18. Kurisawa, M.; Chung, J. E.; Yang, Y. Y.; Gao, S. J.; Uyama, H. *Chem. Commun.* **2005**, *34*, 4312.
19. Sakai, S.; Yamada, Y.; Zenke, T.; Kawakami, K. *J. Mater. Chem.* **2009**, *19*, 230.
20. Jin, R.; Hiemstra, C.; Zhong, Z.; Feijen, J. *Biomaterials* **2007**, *28*, 2791.
21. Sakai, S.; Yamada, Y.; Zenke, T.; Kawakami, K. *J. Mater. Chem.* **2009**, *19*, 230.
22. Orive, G.; Ponce, S.; Hernandez, R. M.; Gascon, A. R.; Igartua, M.; Pedraz, J. L. *Biomaterials* **2002**, *23*, 3825.
23. Heinze, T.; Koschella, A. *Macromol. Symp.* **2005**, *223*, 13.
24. Sakai, S.; Ogushi, Y.; Kawakami, K. *Acta. Biomater.* **2009**, *5*, 554.
25. Sakai, S.; Ito, S.; Ogushi, Y.; Hashimoto, I.; Kawakami, K. *Cellulose* **2008**, *15*, 723.
26. Ogushi, Y.; Sakai, S.; Kawakami, K. *J. Biosci. Bioeng.* **2007**, *104*, 30.
27. Kurisawa, M.; Chung, J. E.; Yang, Y. Y.; Uyama, H. *Chem. Commun.* **2005**, *34*, 4312.
28. Anna, S. L.; Bontoux, N.; Stone, H. A. *Appl. Phys. Lett.* **2003**, *82*, 364.
29. Garstecki, P.; Stone, H. A.; Whitesides, G. M. *Phys. Rev. Lett.* **2005**, *94*, 164501.
30. Gomez-Diaz, D.; Navaza, J. M. *J. Food. Eng.* **2003**, *56*, 387.
31. Garcia-Abuin, A.; Gomez-Diaz, D.; Navaza, J. M.; Quintans-Riveiro, L. C. *Carbohydr. Polym.* **2010**, *80*, 26.
32. Xu, S.; Nie, Z.; Seo, M.; Lewis, P.; Kumacheva, E.; Stone, H. A.; Garstecki, P.; Weibel, D. B.; Gitlin, I.; Whitesides, G. M. *Angew. Chem. Int. Edit.* **2005**, *44*, 724.
33. Seo, M.; Nie, Z.; Xu, S.; Mok, M.; Lewis, P. C.; Graham, R.; Kumacheva, E. *Langmuir* **2005**, *21*, 11614.
34. Nie, Z. H.; Seo, M.; Xu, S. Q.; Lewis, P. C.; Mok, M.; Kumacheva, E.; Whitesides, G. M.; Garstecki, P.; Stone, H. A. *Microfluid Nanofluid* **2008**, *5*, 585.
35. Nisisako, T.; Torii, T.; Higuchi, T. *Chem. Eng. J.* **2004**, *101*, 23.